Chinese Journal of Chemical Engineering 70 (2024) 54–62

Contents lists available at ScienceDirect

Chinese Journal of Chemical Engineering

journal homepage: www.elsevier.com/locate/CJChE

Full Length Article

Experimental study on secondary air mixing along the bed height in a circulating fluidized bed with a multitracer-gas method

Qingyu Zhang [1], Leming Cheng [1,*], Kun Li [1], Qixun Kang [1], Qiang Guo [2], Chaogang Wu [2]

[1] Institute for Thermal Power Engineering, State Key Laboratory of Clean Energy Utilization, Zhejiang University, Hangzhou 310027, China
[2] Dongfang Boiler Group Co. Ltd., Zigong 643001, China

ARTICLE INFO

Article history:
Received 11 December 2023
Received in revised form
2 March 2024
Accepted 7 March 2024
Available online 24 March 2024

Keywords:
Circulating fluidized bed
Secondary air injection
Gas mixing
Multitracer-gas method

ABSTRACT

A multitracer-gas method was proposed to study the secondary air (SA) mixing along the bed height in a circulating fluidized bed (CFB) using carbon monoxide (CO), oxygen (O_2), and carbon dioxide (CO_2) as tracer gases. Experiments were carried out on a cold CFB test rig with a cross-section of 0.42 m × 0.73 m and a height of 5.50 m. The effects of superficial velocity, SA ratio, bed inventory, and particle diameter on the SA mixing were investigated. The results indicate that there are some differences in the measurement results obtained using different tracer gases, wherein the deviation between CO and CO_2 ranges from 42% to 66% and that between O_2 and CO_2 ranges from 45% to 71% in the lower part of the fluidized bed. However, these differences became less pronounced as the bed height increased. Besides, the high solid concentration and fine particle diameter in the CFB may weaken the difference. The measurement results of different tracer gases show the same trends under the variation of operating parameters. Increasing superficial velocity and SA ratio and decreasing particle diameter result in better mixing of the SA. The effect of bed inventory on SA mixing is not monotonic.

1. Introduction

Circulating fluidized bed (CFB) boilers are widely used in gas–solid combustion in industry owing to their advantages of low pollutant emissions, wide fuel adaptability, and intensive gas–solid mixing [1]. Secondary air (SA), which is commonly used in CFB boilers, has an important effect on gas mixing and oxygen concentration distribution in the furnace, eventually affecting combustion processes and NO_x/N_2O emissions [2–6]. As the CFB boiler's capacity and steam parameters increase, SA injection and mixing in the furnace become one of the most important issues due to the increase in cross-sectional area of the furnace [1].

The injection of SA influences the gas–solid hydrodynamics in a CFB. Researches were conducted through both experiments and numerical simulations, including in a fluidized bed test rig [7–16] and large-scale CFB boilers [17–19]. It has been established that the SA velocity affects the penetration depth of SA in a power law correlation, which is also influenced to some extent by the primary air (PA) flow [7,8]. Specifically, the penetration depth of the SA increases with the SA velocity and decreases with the PA velocity and solid concentration [14,18]. However, the studies have largely focused on the SA mixing at the SA injection area without significant consideration for the subsequent gas mixing along the height of the furnace.

A gas tracer method was typically utilized in the study of gas mixing in a fluidized bed, and the use of a single tracer gas is common in such studies [20–32]. The tracer gas was injected into the fluidized bed, and its concentration distribution was measured through a sampling probe. This enabled researchers to determine the gas mixing behavior within the fluidized bed and explore how it is affected by factors such as solid concentration [21,22], superficial velocity [24,25], and particle properties [29,32] in the fluidized bed. Additionally, the method has been applied to explore the influence of SA ratio and SA nozzle type on axial and radial gas mixing, revealing that gas mixing increases with a higher SA ratio [33–35].

Among the researches, gases including CO_2 (relative molecular mass 44) [23,29–32,34,35], He (relative molecular mass 4) [24,25,28], H_2 (relative molecular mass 2) [26], Ar (relative molecular mass 40) [22], SF_6 (relative molecular mass 146) [21], and some hydrocarbons including CH_4 (relative molecular mass 16) [20]

* Corresponding author.
E-mail address: lemingc@zju.edu.cn (L. Cheng).

https://doi.org/10.1016/j.cjche.2024.03.003
1004-9541/

and C_3H_6 (relative molecular mass 42) [27] have been used as tracer gases. CO_2, as a stable and safe gas, was commonly used as a tracer gas in the experiments. However, different gases with different properties occur during coal combustion in a CFB boiler. The mixing characteristics of those gases in the furnace are different due to their different densities, viscosities and diffusivities. Their different mixing will influence the gas distribution and,thus, the combustion, heat transfer and emissions in the furnace. The gases mix and inject differently, even though they have the same velocity. Namkung and Kim [36] reported deviations in results when using CO_2 compared to He. It is valuable to test the hydrodynamics with different tracer gases. Hence, this study proposes using multitracer gases to investigate gas mixing.

To comprehensively study the SA mixing characteristics in a CFB furnace, it is essential to examine not only the SA injection area but also its distribution and effects in the subsequent areas along the height of the furnace. Additionally, it is important to investigate the mixing characteristics of various gas phases along the height of the CFB furnace following SA injection. Although there have been some studies conducted on SA injection, the aforementioned topics have not been extensively studied in the literature and hence require further investigation.

In this study, a novel multitracer-gas method was employed to investigate the injection and mixing of SA along the bed height in a CFB. The tracer gases, composed of carbon monoxide (CO), oxygen (O_2) and carbon dioxide (CO_2) were fed into the CFB through a SA nozzle. The concentrations of these gases were measured instantaneously and simultaneously at multiple points along the height of the riser. The effects of superficial velocity (u_0), secondary air ratio ($SAR = Q_{SA}/(Q_{PA} + Q_{SA})$), bed inventory (quantified by the static bed material height, H_0) and particle diameter (d_p) on the injection and mixing of SA were studied.

2. Experimental

2.1. The multitracer-gas method

The multitracer-gas method is based on the fundamentals of the conventional gas tracer method, with the addition of utilizing multiple component gases as the tracer gas. This methodology confers the ability to study the mixing of gases with different characteristics, thereby providing distinct advantages.

Multiple gases were selected with consideration given to the density of the tracer gas and the measurement accuracy of the tracer gas comprehensively. These gases were premixed with the SA prior to entering the furnace. The mixing characteristics of the gases were studied by measuring the concentration profile of the tracer gas in the riser.

As mentioned above, a tracer gas should have similar physical characteristics to the operating medium to ensure similar hydrodynamics. For representativeness of tests run with air at room temperature, the relative molecular mass of a tracer gas should be close to 29, which is the relative molecular mass of air. By using the multitracer-gas method, three gases, CO, O_2 and CO_2, were selected as the tracer gases in the tests. Among them, CO has a relative molecular mass closest to that of air and serves as a monitor for measurement accuracy. O_2 has a slightly higher relative molecular mass than air and is the main gas involved in combustion in the SA. A higher O_2 flow rate was used to ensure a noticeable response from the gas sensors when using O_2 as a tracer gas. CO_2 has a larger relative molecular mass than air and is often used for gas tracing and applied as a reference in this study. At room temperature, these three gases are stable and do not react with each other.

2.2. Test rig and experimental conditions

Fig. 1 shows the schematic of the CFB test rig with a multitracer-gas measuring system. It is composed of a CFB cold test rig, an air supply system, an induced air system, a multitracer-gas measurement system, and a data acquisition system. The CFB cold test rig consists of a riser with a pant leg at its bottom, as well as six cyclones and their corresponding solid return system. The riser has a cross-sectional area of 0.42 m × 0.73 m and a height of 5.50 m. At the bottom of the riser, the internal wall of the pant leg is 1 m high above the air distributors.

The air blower supplied both PA and SA. The PA entered the bed through the air distributors at the bottom to fluidize the solid bed material, while the SA was injected into the bed through the SA nozzles located around the riser. The gas–solid flow moved through the furnace and exited from the upper part of the riser before being separated in the cyclones. The separated gas was then released into the environment after passing through a bag filter, while the separated solid particles were returned to the bottom of the riser through the standpipes and loop seals. The flow rates of the PA and SA were measured using airfoil flowmeters and rotameters, respectively.

Fig. 2 shows the arrangement of the SA nozzles. The pant-leg contains two layers of SA nozzles on each side of its internal wall, located at heights of 0.40 m and 0.60 m. Additionally, one layer of SA nozzles is present on each side of the external wall of the pant leg at a height of 0.60 m. Each layer of SA nozzles has eight nozzle units.

In order to state this clearly, the SA nozzles were identified and differentiated according to their height and position on the pant leg. The nozzles on the external surface were referred to as outside upper secondary air (OUSA), while those on the internal upper layer were called inner upper secondary air (IUSA). Furthermore, the nozzles located on the internal lower layer were named inner lower secondary air (ILSA). In addition, the central SA nozzles were identified as the fourth nozzles of each layer from the front wall. To avoid the effect of the riser wall, during the tests, the multitracer-gas was injected into the riser through the central SA nozzle of OUSA on the left wall.

Three sizes of glass beads were used as bed material in the experiments. Their properties are shown in Table 1. The glass bead II with a mean diameter of 0.12 mm was used as the bed material in most tests. The other two types of glass beads were used in the

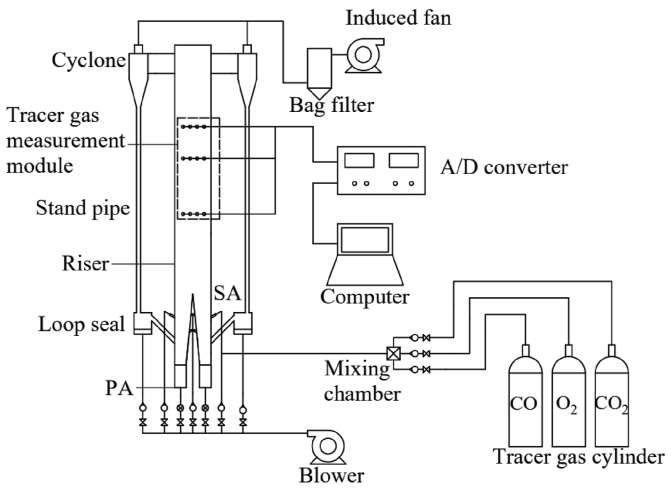

Fig. 1. Schematic of the CFB test rig with a multitracer-gas measuring system.

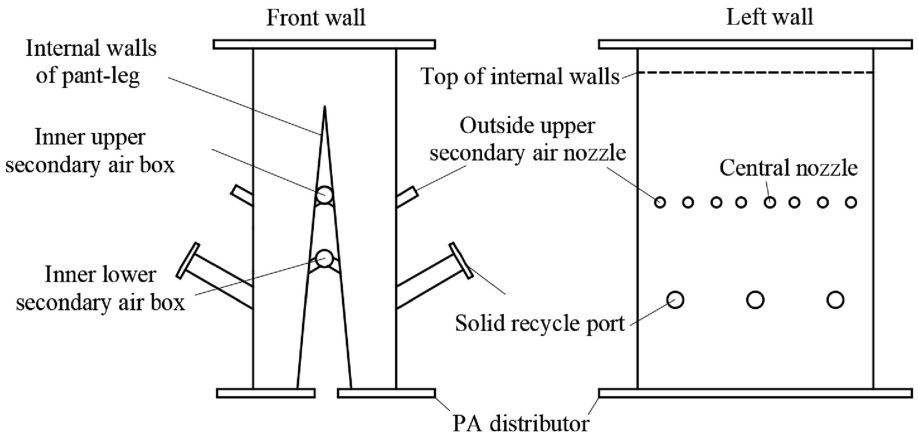

Fig. 2. SA nozzles arrangement.

Table 1
Properties of bed material

Parameter	Glass bead I	Glass bead II	Glass bead III
Particle mean diameter, d_p/mm	0.10	0.12	0.15
Particle density, ρ_s/kg·m^{-3}	2350	2350	2350
Particle terminal velocity, u_t/m·s^{-1}	0.67	0.79	0.96
Minimum fluidization velocity, u_{mf}/m·s^{-1}	0.007	0.011	0.017

comparative experiments. In addition, the operating parameters of the experiments are given in Table 2.

2.3. The multitracer-gas measurement system and data processing

The multitracer-gas measurement system consists of three parts: gas supply, gas injection and gas detection. The multitracer gases, provided by gas cylinders in a ratio of CO:O_2:CO_2 = 1:10:2, were mixed with SA and then injected into the riser through the SA nozzle. The ratio of multi-tracer gases was selected mainly considering the measuring responses and range of the gas sensors. Fig. 3 shows the SA nozzle with the multi-tracer-gas injection system. During the tests of variable operating parameters, the gas supply system maintained a constant supply ratio of multi-tracer gases at the SA nozzle while also controlling the concentrations to remain consistent, thus avoiding errors caused by deviations in the initial concentrations.

In the experiments, the gas detection consists of three levels of measurement points along the bed, with a total of 12 points. A probe was installed at each point to measure the concentrations of trace gases using CO, O_2 and CO_2 gas sensors. The product data sheets for the gas sensors are presented in Table 3. These sensors were uniformly installed on the probes and were able to move horizontally at the measurement level with the probes. The probes were placed above the central SA nozzle during the tests, as shown in Fig. 4(a). In addition, as shown in Fig. 4(b), the measurement levels were positioned at heights (h) of 2.05 m, 3.45 m and 4.25 m above the air distributors, corresponding to relative bed heights of h/H 0.37, 0.63 and 0.77, respectively. Here, H represents the height of the riser, which is measured to be 5.50 m. The distance between the four measurement points of each level and the riser's left wall is 61, 161, 261 and 361 mm, respectively.

The gas sensor signals were acquired using an A/D converter (Agilent 34970A) and then transferred to the data acquisition system simultaneously. The sensors were calibrated before the measurements.

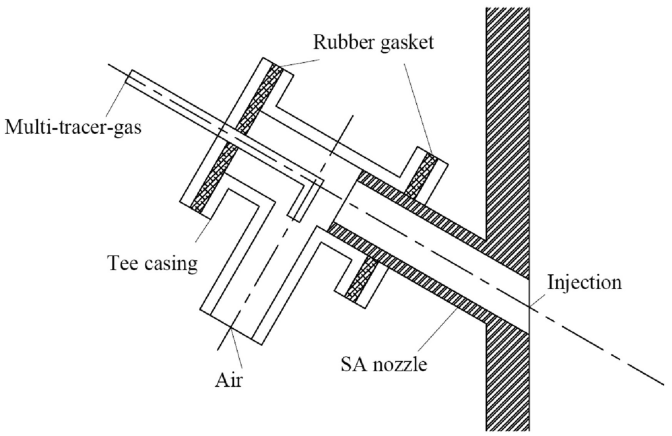

Fig. 3. SA nozzle with multi-tracer-gas injection.

Table 3
Product data sheets of the gas sensors

Gas sensors	Model	Manufacturer	Measurement range	Resolution
CO	4CO-500	Honeywell	0–500 ml·m^{-3}	1 ml·m^{-3}
O_2	4OXV	CITICEL	0%–25% (vol)	0.02% (vol)
CO_2	G8 (S)	AEGIS	0–2000 ml·m^{-3}	5 ml·m^{-3}

Table 2
Values of the operating parameters

Parameter	Value
Superficial velocity, u_0/m·s^{-1}	1.10, 1.25, 1.40, 1.55, 1.70
Secondary air ratio	0.35, 0.40, 0.45, 0.50, 0.55
Particle mean diameter, d_p/mm	0.10, 0.12, 0.15
Static bed material height, H_0/mm	200, 300, 400

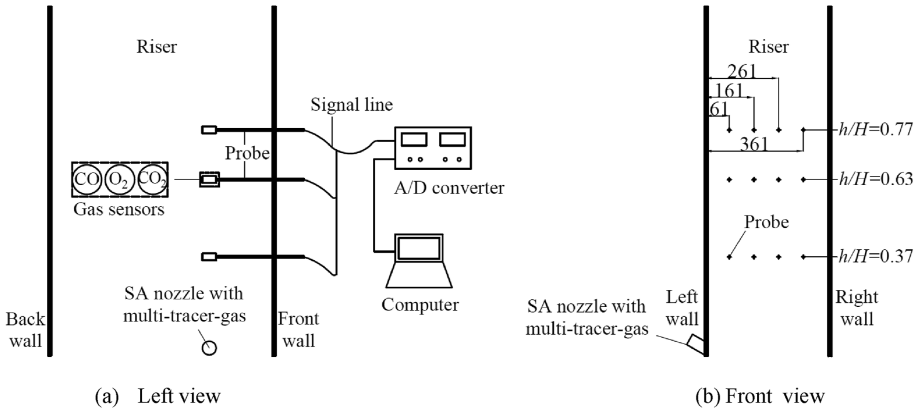

Fig. 4. Schematic of multitracer-gas measurement system.

After penetrating into the riser, the tracer gases mixed with the air. The dimensionless concentration expression of a certain tracer gas (one in the multitracer gases) at any point of measurement in the riser can be determined as follows:

$$C_i = \frac{C - C_0}{C_2 - C_0} \tag{1}$$

where C_i is the dimensionless gas concentration at the measuring point i, C_0 and C are the certain tracer gas concentrations at the measuring point i before and after the injection of multi-tracer-gas, respectively. C_2 is the tracer gas concentration at the SA nozzle, and it is calculated as follows:

$$C_2 = \frac{Q_{t,g} + Q_{sa,g}}{Q_t + Q_{sa}} \tag{2}$$

where Q_t is the total flow rate of multi-tracer-gas in the SA nozzle, Q_{sa} is the flow rate of SA air in the SA nozzle, $Q_{t,g}$ is the flow rate of the certain tracer gas, and $Q_{sa,g}$ is the flow rate of the certain tracer gas in the SA air. The value of $Q_{sa,g}$ depends on the certain tracer gas; when the certain tracer gas is O_2 or CO_2, $Q_{sa,g}$ is nonzero due to the presence of these gases in the SA air. However, when a certain tracer gas is CO, $Q_{sa,g}$ is zero.

In this study, a parameter named the lateral diffusion displacement of the tracer gas was proposed to characterize the SA movement and mixing along the bed height. Fig. 5 gives the schematic of the lateral diffusion displacement, which is defined as the horizontal displacement of the local maximum tracer gas concentration measured at a certain bed height, denoted as L_x, as shown in Fig. 5. It is a result of the SA injecting velocity, its diffusion, and the operating parameters of the system.

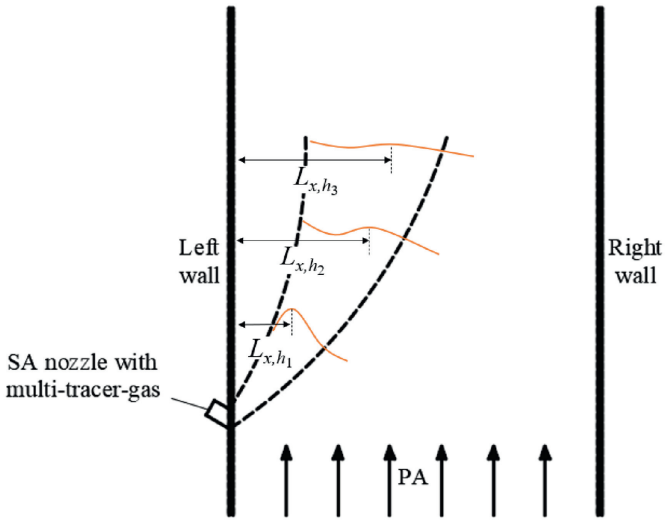

Fig. 5. Schematic of the lateral diffusion displacement.

In the experiments, the concentrations of tracer gases at various measuring points were recorded, and their profiles at the same bed height were obtained. Thus, the lateral diffusion displacement can be determined according to the position of the local maximum point of the tracer gas concentration. In the lower part of the fluidized bed, the largest value in the concentration profile can be observed as the local maximum. However, in the middle or upper part of the fluidized bed, the maximum value of the concentration profile is not well defined due to the mixing of the SA with the main gas–solid flow. In this case, the position with a slope of zero in the concentration profile is chosen as the local maximum. As shown in Fig. 5, L_{x,h_1}, L_{x,h_2} and L_{x,h_3} represent the lateral diffusion displacement at different bed heights, respectively. To quantify the lateral diffusion displacement dimensionally, the dimensionless lateral diffusion displacement, L_{xi}, was introduced.

$$L_{xi} = \frac{L_x}{L} \tag{3}$$

where L ($L = 0.42$ m) is the depth of the riser.

The uncertainties of the measurements on the SA lateral diffusion displacements by multi-tracer gases were mainly caused by the errors in gas concentrations measured by the tracer gas sensors. To avoid this error, each measurement was carried on in the steady state and repeated three times. The uncertainties in the measurements were considered in two aspects: the repeatability of the experiments and the accuracy of the gas sensors. The resolutions for CO, O_2 and CO_2 gas sensors were ± 1 ml·m^{-3}, $\pm 0.02\%$ (vol) and ± 5 ml·m^{-3}, respectively (Table 3). The standard uncertainties for the multitracer gas sensors were $\pm 0.2\%$, $\pm 0.08\%$ and $\pm 0.25\%$, considering the measurement ranges, and they may be neglected. The uncertainties of the repeatability of the SA lateral diffusion displacements were represented by the standard deviations in the mean experimental measurements. The standard uncertainties for CO, O_2 and CO_2 were ± 2 mm, ± 5 mm and ± 3 mm, respectively. In particular, the standard uncertainties for the multitracer gas sensors were $\pm 0.48\%$, $\pm 1.19\%$ and $\pm 0.71\%$ considering the depth of the riser. These values illustrate the good repeatability of the measurements. Additionally, the mean SA lateral diffusion displacements were used in the result analysis.

3. Results and Discussion

3.1. Mixing characteristics of multitracer gases

3.1.1. Distributions of multi-tracer gases along the bed height

Fig. 6 shows the horizontal distributions of the multitracer gas dimensionless concentrations in the riser at three different heights. The test was conducted under the conditions of $u_0 = 1.7\ \mathrm{m\cdot s^{-1}}$, SAR = 0.55, $H_0 = 200$ mm and $d_p = 0.12$ mm. It can be seen that the results measured by the three tracer gases show a similar trend. As the height increases, the distributions of multi-tracer gas concentrations become more uniform, and the largest concentration values become less clear. Specifically, at $h/H = 0.37$, there are the largest concentrations located close to the SA nozzle, while the center region of the furnace shows more multitracer gas concentrations at $h/H = 0.63$ and 0.77. This phenomenon illustrates that supplying SA to one side of the furnace can effectively support oxygen supply and extend it at least to the middle of the furnace. Additionally, the uniform distributions of tracer gas concentrations in the upper part of the riser can be attributed to the intensified mixing that occurs in this region of the fluidized bed. Besides, there are notable differences in the distributions of multitracer gases, particularly with CO_2 compared to O_2 and CO. The lateral diffusion displacement of the SA obtained by the CO_2 local maximum concentration (L_{x,CO_2}) is different from that of O_2 (L_{x,O_2}) and CO ($L_{x,CO}$), and the concentration distributions measured by O_2 and CO are relatively similar.

3.1.2. Lateral diffusion displacements of multi-tracer gases along the bed height

The lateral diffusion displacements of SA along the height of the riser, as determined by the distribution of tracer gas concentration, are summarized in Fig. 7. The results clearly show that the lateral diffusion displacement of SA increases as the height increases, with a smoother variation in the h/H range of 0.63–0.77. At higher levels of the riser, particularly at $h/H = 0.77$, there is a relatively smaller difference in the displacements among the tracer gases compared to lower levels. These findings indicate that gases become more thoroughly mixed as the bed height increases and will reach a state of mixing balance in the upper region.

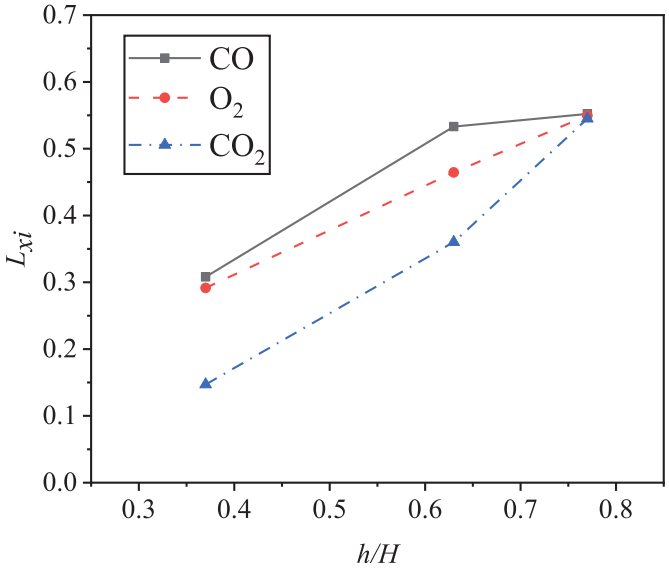

Fig. 7. Lateral diffusion displacements of multitracer gases along the bed height.

3.2. Secondary air mixing characteristics with multitracer gas method

3.2.1. Effect of superficial velocity

Fig. 8 illustrates the lateral diffusion displacements of multi-tracer gases at different bed heights and superficial velocities in the range of 1.10–1.70 $\mathrm{m\cdot s^{-1}}$. The lateral diffusion displacement of each tracer gas increases slightly with the increase of superficial velocity. In the tests, the SAR was kept constant while the superficial velocity varied. As the superficial velocity increased, the flow of SA increased, promoting SA injection into the bed. However, the solid suspension density in the SA injection region also increased as the flow of PA increased, impeding SA injection. As a result, the lateral diffusion displacement of SA shows a slight increase with the superficial velocity.

The variations of lateral diffusion displacement with superficial velocities measured by multitracer gases are different. The lateral diffusion displacements measured by O_2 and CO are very close to each other but slightly deeper than those of CO_2. This difference is most notable at $h/H = 0.37$, remains consistent under different superficial velocity test conditions, and gradually converges as the bed height increases. This may imply the function of different gas characteristics. Notably, at $h/H = 0.37$, when the superficial velocity increases to 1.4 $\mathrm{m\cdot s^{-1}}$, the lateral diffusion displacements measured by CO and CO_2 increase significantly. This may be due to the transition of the gas–solid flow regime in the riser [28]. The lighter CO is most sensitive to this change.

3.2.2. Effect of secondary air ratio

Fig. 9 displays the lateral diffusion displacements of multitracer gases at different heights with SARs of 0.35, 0.40, 0.45, 0.50 and 0.55. The results illustrate a positive correlation between the lateral diffusion displacements of each tracer gas and SAR. During the tests, the SAR was changed by reducing the SA flow rate while

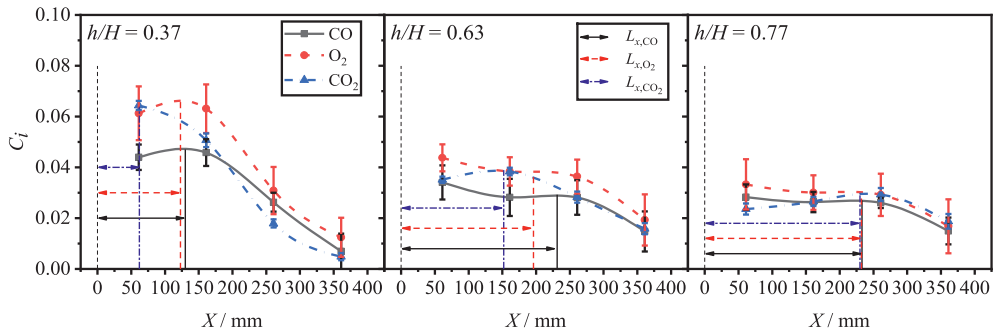

Fig. 6. Distributions of multitracer gases along the bed height.

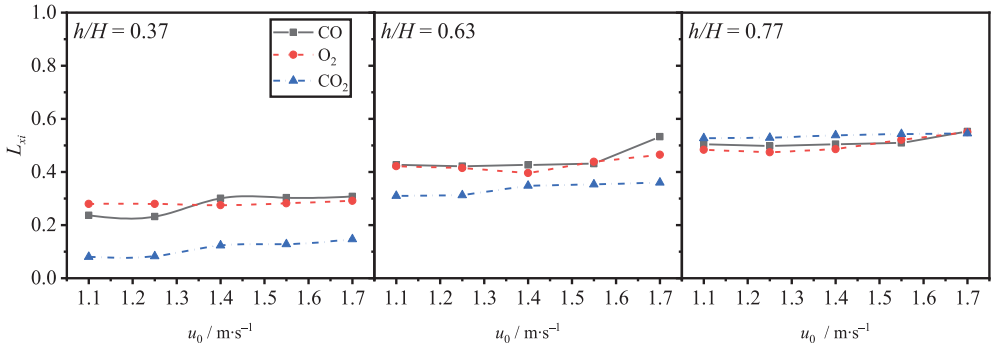

Fig. 8. Variations of SA lateral diffusion displacement with superficial velocity.

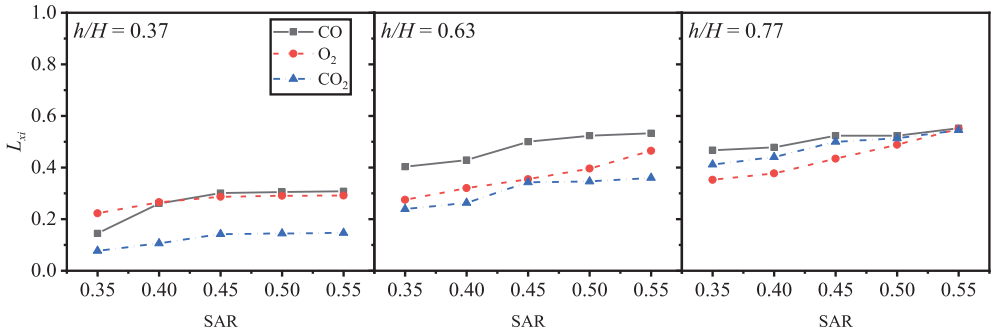

Fig. 9. Variations of SA lateral diffusion displacement with SAR.

keeping the PA flow rate constant. As SAR increases, the SA velocity also increases, resulting in a significant diffusion kinetic energy of SA and deeper lateral diffusion displacement in the fluidized bed, which leads to better mixing of gases.

The variations of lateral diffusion displacement with SAR of multi-tracer gases in the tests are similar. At $h/H = 0.37$, the relationship between the lateral diffusion displacement of SA and SAR does not follow a linear trend, but rather exhibits a power exponential relationship, in agreement with findings reported by Chen *et al.* [8]. This variation is more noticeable in the measurement results of CO. Moreover, it should be noted that SA mixing is still affected by the SAR in the upper region, though the effect is less than that in the lower bed.

3.2.3. *Effect of bed inventory*

Except for the operating parameters related to gas velocity, solid concentration also affects SA mixing in the fluidized bed. Fig. 10 reveals the differences in lateral diffusion displacements of multi-tracer gases at varying bed heights and different bed inventories corresponding to static bed material heights of 200 mm, 300 mm and 400 mm. The results show that the lateral diffusion displacement of each tracer gas increases at first and then decreases with the increase of the bed inventory. Notably, the lateral diffusion displacements decrease clearly when the static bed material height increases to 400 mm, especially at $h/H = 0.37$.

In a fluidized bed, the increase of bed inventory has two effects on the SA mixing. On the one hand, the increasing of the gas–solid suspension density, caused by increasing bed inventory, elevates the lateral diffusion resistance of SA injection [18]. On the other hand, an increase in bed inventory may intensify turbulence in the fluidized bed, thereby enhancing gas mixing [37]. The effect of bed inventory on the SA mixing in the fluidized bed is the comprehensive result of the above two factors. When the bed inventory is low, the SA mixing is mainly affected by the enhancement of the turbulence intensity, thus the SA mixing is enhanced. When the bed inventory is high, the higher gas–solid suspension density will have a strong inhibitory effect on the lateral diffusion of the SA. Hence, the SA mixing is weakened. In conclusion, the lateral

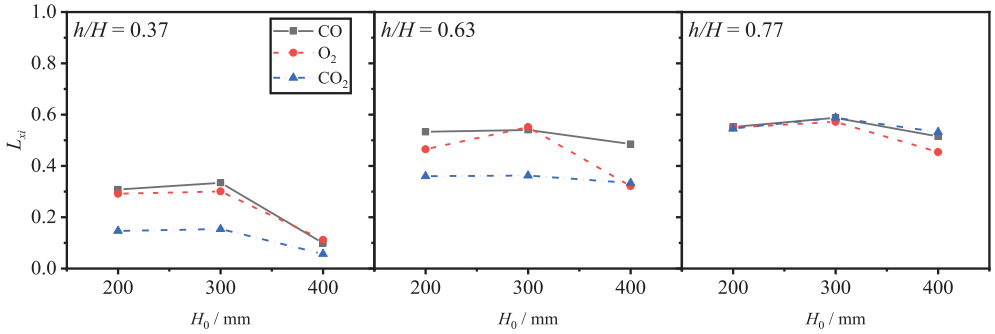

Fig. 10. Variations of SA lateral diffusion displacement with bed inventory.

diffusion displacement of the SA increases at first and then decreases as the bed inventory increases.

The variations of lateral diffusion displacement with the bed inventory of multitracer gases show the same trend. The solid concentration in the riser is the highest when the static bed material height is 400 mm, and the lateral diffusion displacements of SA measured by different tracer gases are the closest at $h/H = 0.37$. This can be attributed to the fact that the effect of the solid concentration on the mixing of different tracer gases is more substantial in the lower part of the fluidized bed than that of the tracer gas density.

3.2.4. Effect of particle diameter

Fig. 11 shows the lateral diffusion displacements of multi-tracer gases at different heights, considering particle diameters of 0.10, 0.12 and 0.15 mm. The results indicate that the lateral diffusion displacement of each tracer gas increases with decreasing particle diameter, presumably due to enhanced turbulence in the bed when particle diameter is finer [32]. This trend is more obvious in the upper part of the fluidized bed. These observations are consistent with the application of fluidization pattern reconstruction in the design of CFB boilers [38,39]. In addition, when the particle diameter is 0.10 mm at $h/H = 0.77$, the differences in lateral diffusion displacements measured by different tracer gases are relatively small. This finding implies that gas mixing in the upper portion of the fluidized bed is more influenced by gas–solid flow turbulence than the gas density.

3.2.5. Deviations in multitracer gases

According to the definition of SA lateral diffusion displacement, the data obtained from the tests using the multitracer-gas method were summarized and processed in a nondimensional manner.

To compare the results obtained by different tracer gases, the deviations between two gases were calculated using the following equation:

$$\mathrm{Dev} = \frac{L_{xi,\max} - L_{xi,\min}}{L_{xi,\max}} \times 100\% \tag{4}$$

where $L_{xi,\max}$ represents the maximum dimensionless lateral diffusion displacement between the tracer gases, while $L_{xi,\min}$ represents the minimum dimensionless lateral diffusion displacement.

Fig. 12 illustrates the deviations in the lateral diffusion displacements of multitracer gases. The deviations are more pronounced at $h/H = 0.37$ in the dense lower part of the fluidized bed, particularly between CO_2 and the other two gases. The deviation is 42% to 66% between CO_2 and CO, and 45% to 71% between CO_2 and O_2. However, when $h/H > 0.37$ in the dilute upper part of the fluidized bed, the deviations in lateral diffusion displacements obtained by multitracer gases become notably smaller. The maximum

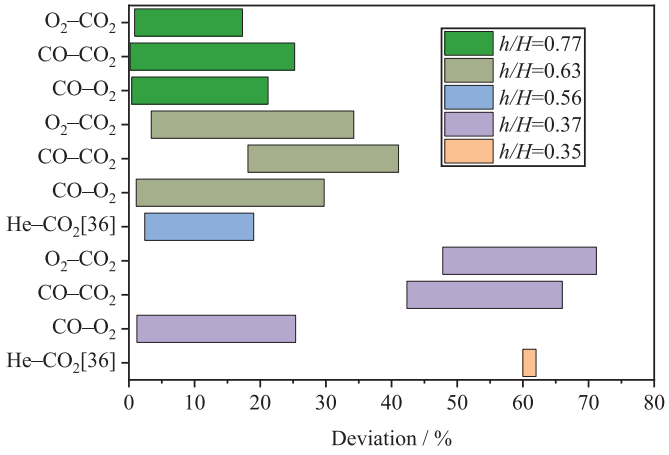

Fig. 12. Deviations between results obtained by multitracer gases.

deviation is 41% between CO_2 and O_2 at $h/H = 0.63$. Similar deviations were reported by Namkung and Kim [36] in their study of gas mixing, as illustrated in Fig. 12. The deviation between CO and O_2 remained within 30% at any height of the fluidized bed.

Based on the test results, an empirical formula for the SA lateral diffusion displacements of multitracer gases is summarized and proposed. Previous works indicate that the mixing of SA in a fluidized bed is affected by superficial velocity (u_0), secondary air ratio (SAR), bed inventory (H_0), and particle diameter (d_p) [23,24,29,34]. In addition, this work obtains results on the SA lateral diffusion along the bed height with different gases of different properties. Hence, two more important factors, the bed height and the tracer gas diffusivity (D_t, Table 4), are raised to be part of the dimensionless group of the empirical formula. Therefore, the empirical formula describing the SA lateral diffusion displacement is summarized as follows according to the test results:

$$L_{xi} = 16.543\left(\frac{D_t}{u_{mf}L}\right)^{1.270}\left(\frac{u_0}{u_{mf}}\right)^{0.355} \times \mathrm{SAR}^{0.722}\left(\frac{H_0}{H}\right)^{-0.369}\left(\frac{d_p\rho_s}{L\rho_g}\right)^{2.860}\left(\frac{h}{H}\right)^{1.278} \tag{5}$$

Table 4
Gas diffusivity (atmospheric pressure, 25 °C) [40]

	$D_t \times 10^4/\mathrm{m^2\cdot s^{-1}}$
CO–air	0.212
O_2–air	0.213
CO_2–air	0.162

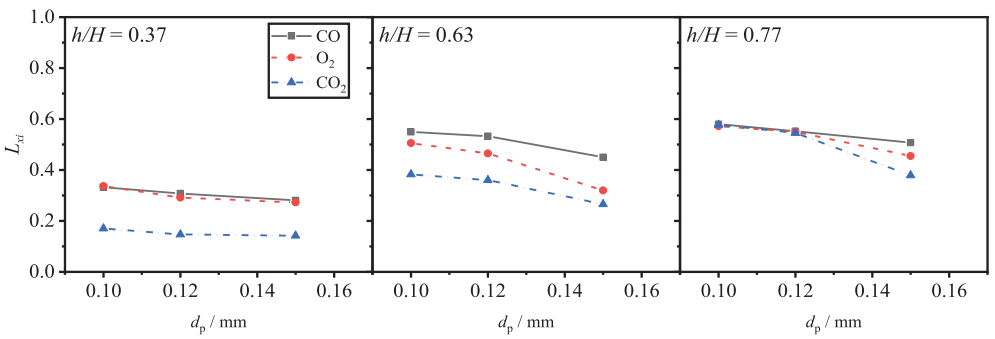

Fig. 11. Variations of SA lateral diffusion displacement with particle diameter.

where u_0/u_{mf} is the ratio of superficial velocity to minimum fluidization velocity and represents the dimensionless superficial gas velocity, SAR is the secondary air ratio and represents the dimensionless secondary air flow rate, H_0/H is the ratio of static bed material height to bed height and represents the dimensionless bed inventory, $d_p\rho_s/L\rho_g$ (ρ_g is the air density, 1.18 kg·m^{-3}) is the dimensionless representation of particle diameter, h/H represents the relative bed height, and $D_t/u_{mf}L$ is the ratio of gas diffusivity to the minimum fluidization velocity and depth of the riser, and represents the dimensionless tracer gas diffusivity.

Fig. 13 compares the results obtained from the empirical formula with the corresponding test data measured by the multitracer gases. The average differences between empirical and measured values for CO, O_2 and CO_2 are 13.16%, 14.41% and 15.33%, respectively, with an overall average difference of 14.30%. It is evident that the dimensionless lateral diffusion displacements measured by different tracer gases are different. CO_2 spreads more weakly compared to O_2 and CO. This can be understood due to its higher relative molecular mass and smaller diffusivity. A very important conclusion may be drawn that gases generated in a CFB furnace have different mixing characteristics due to their different physical properties. Different gases have different densities, viscosities, and diffusivities, and these factors influence their mixing and diffusion characteristics in the gas–solid flow in the CFB. In the lower dense phase, the high solid concentration is unfavorable to gas mixing. CO_2, having a larger relative molecular mass, results in a smaller lateral diffusion displacement than that of CO and O_2. Besides, according to Table 4, the diffusivity of CO_2 is significantly smaller than that of CO and O_2. This also has a negative influence on CO_2 mixing. In the upper dilute phase, the solid concentration is lower, and the small amount of particle exchange existing in the gas–solid flow in the fluidized bed promotes the gas mixing [37]. The lateral diffusion displacements of multitracer gases are relatively closer. In summary, the properties of tracer gases may need to be considered when addressing the complex issues of gas mixing in a CFB furnace. The empirical formula provides references for studying gas mixing along the bed height in a CFB and tests using one or more tracer gas methods.

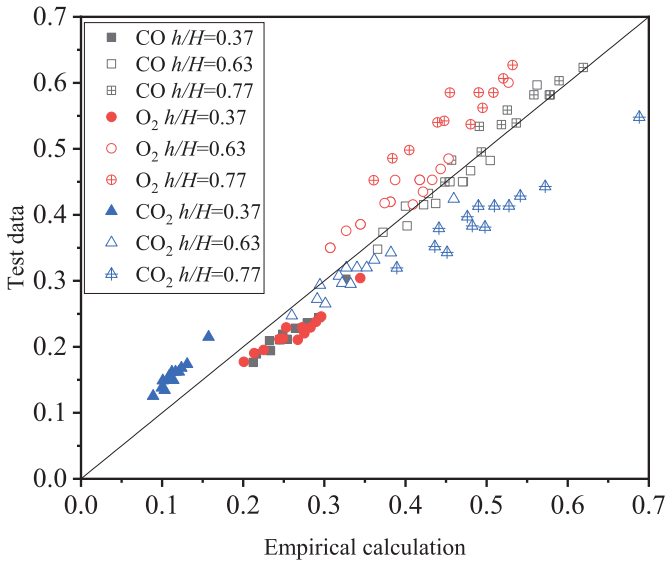

Fig. 13. Comparisons between empirical calculations and test data.

4. Conclusions

A multitracer-gas method was put forward to investigate the SA mixing characteristic along the bed height in a CFB. Experiments were conducted to investigate the effects of superficial velocity, SAR, bed inventory, and particle diameter on the mixing of SA. The main conclusions are as follows:

(1) The multitracer-gas method can be used to measure the mixing of gases with different characteristics in a fluidized bed. It is effective and may serve as a reference for experiments that involve measuring the hydrodynamics of different gases simultaneously.
(2) Differences were observed during experiments measuring the mixing of SA in a CFB using multitracer gases. The results obtained from CO and O_2 gases are more consistent with each other compared to those obtained from CO_2. Particularly, the deviations are 42%–66% in CO_2 and CO and 45%–71% in CO_2 and O_2 in the lower part of the fluidized bed. It is possible that these differences may be attenuated by the higher solid concentration and finer particle diameter in the CFB.
(3) The variation trends of SA mixing as measured by multitracer gases are consistent. The increasing of superficial velocity and SAR have a positive effect on the SA mixing. However, a larger bed inventory and particle size hinder the SA mixing. The combined results may be expressed by the empirical formula for multi-tracer gases.

Declaration of Interest

The authors declare that they have no known competing financial interests or personal relationships that could have appeared to influence the work reported in this paper.

Acknowledgement

This work was financed by the Key Project of the National Research Program of China (2020YFB0606201).

Nomenclature

C	gas concentration at measuring point i after the injection of multi-tracer-gas, ml·m^{-3}
C_i	dimensionless gas concentration at measuring point i
C_0	gas concentration at measuring point i before the injection of multi-tracer-gas, ml·m^{-3}
C_2	gas concentration at the secondary air nozzle, ml·m^{-3}
D_t	gas diffusivity, m^2·s^{-1}
Dev	deviation between tracer gases
d_p	particle mean diameter, mm
H	height of the riser, m
H_0	static bed material height, mm
h	height of the measuring level, m
h/H	relative bed height
L	depth of the riser, m
L_x	lateral diffusion displacement of secondary air, m
L_{xi}	dimensionless lateral diffusion displacement of secondary air
Q_{PA}	flow rate of primary air, m^3·h^{-1}
Q_{SA}	flow rate of secondary air, m^3·h^{-1}
Q_{sa}	flow rate of secondary air in a secondary air nozzle, m^3·h^{-1}

$Q_{sa,g}$ flow rate of a certain tracer gas in secondary air, $m^3 \cdot h^{-1}$
Q_t flow rate of multi-tracer-gas, $m^3 \cdot h^{-1}$
$Q_{t,g}$ flow rate of a certain tracer gas in multi-tracer-gas, $m^3 \cdot h^{-1}$
u_{mf} minimum fluidization velocity, $m \cdot s^{-1}$
u_t particle terminal velocity, $m \cdot s^{-1}$
u_0 superficial velocity, $m \cdot s^{-1}$
ρ_g air density, $kg \cdot m^{-3}$
ρ_s particle density, $kg \cdot m^{-3}$

References

[1] L.M. Cheng, J.Q. Ji, Y.J. Wei, Q.H. Wang, M.X. Fang, Z.Y. Luo, M.J. Ni, K.F. Cen, A note on large-size supercritical CFB technology development, *Powder Technol.* 363 (2020) 398–407.
[2] K. El Sheikh, M.J.H. Khan, M. Diana Hamid, S. Shrestha, B.S. Ali, G.A. Ryabov, L. A. Dolgushin, M.A. Hussain, T.V. Bukharkina, E.A. Gorelova, Advances in reduction of NO and N_2O emission formation in an oxy-fired fluidized bed boiler, *Chin. J. Chem. Eng.* 27 (2) (2019) 426–443.
[3] J.Q. Ji, L.M. Cheng, Y.J. Wei, J.F. Wang, X.Y. Gao, M.X. Fang, Q.H. Wang, Predictions of NO_x/N_2O emissions from an ultra-supercritical CFB boiler using a 2-D comprehensive CFD combustion model, *Particuology* 49 (2020) 77–87.
[4] H.P. Liu, H.W. Sun, Y. Bi, C.X. Jia, L. Zhang, Y.L. Li, H. Qin, Q. Wang, Effect of secondary air on NO emission in a 440 t/h circulating fluidized bed boiler based on CPFD method, *Particuology* 83 (2023) 18–31.
[5] J. Yan, X. Zheng, X.F. Lu, Z. Liu, X.C. Fan, Enhanced combustion behavior and NO*x* reduction performance in a CFB combustor by combining flue gas recirculation with air-staging: Effect of injection position, *J. Energy Inst.* 96 (2021) 294–309.
[6] X.W. Ke, M. Engblom, H.R. Yang, A. Brink, J.F. Lyu, M. Zhang, B. Zhao, Prediction and minimization of NO*x* emission in a circulating fluidized bed combustor: A comprehensive mathematical model for CFB combustion, *Fuel* 309 (2022) 122133.
[7] J.H. Chen, X.F. Lu, H.Z. Liu, J. Liu, The effect of solid concentration on the secondary air-jetting penetration in a bubbling fluidized bed, *Powder Technol.* 185 (2) (2008) 164–169.
[8] J.H. Chen, X.F. Lu, H.Z. Liu, J. Liu, Experimental study and numerical simulation of secondary air's jet length in circulating fluidized beds, *J. Power Eng.* 27 (6) (2007) 895–898.
[9] C.S. Hu, K. Luo, M.M. Zhou, J.J. Lin, D.L. Kong, J.R. Fan, Influences of secondary gas injection pattern on fluidized bed combustion process: A CFD-DEM study, *Fuel* 268 (2020) 117314.
[10] T.W. Li, K. Pougatch, M. Salcudean, D. Grecov, Mixing of secondary gas injection in a bubbling fluidized bed, *Chem. Eng. Res. Des.* 87 (11) (2009) 1451–1465.
[11] Z.Y. Wang, S.Z. Sun, X.Y. Meng, S.H. Wu, Y.F. Tan, Effects of coarse particle addition on solids distribution of CFB with air-staging, in: 2011 International Conference on Computer Distributed Control and Intelligent Environmental Monitoring, Changsha, China, 2011, pp. 1190–1193.
[12] Z.Y. Wang, Y.F. Tan, N.B. Zhao, S.Z. Sun, S.H. Wu, Experimental study on the penetration model of secondary air injection in CFB, in: 2011 Asia-Pacific Power and Energy Engineering Conference, Wuhan, China, 2011, pp. 1–4.
[13] Z.Y. Wang, S.Z. Sun, H. Chen, S.H. Wu, Y.F. Tan, Experimental research on the corner secondary air injection of square circulating fluidized bed, in: 2010 Asia-Pacific Power and Energy Engineering Conference, Chengdu, China, 2010, pp. 1–4.
[14] J.H. Yang, H.R. Yang, G.X. Yue, Experimental study on secondary air jet penetration in circulating fluidized bed, *J. Power Eng.* 28 (4) (2008) 509–513.
[15] W.J. Zheng, M. Zhang, Y. Zhang, J.F. Lyu, H.R. Yang, The effect of the secondary air injection on the gas–solid flow characteristics in the circulating fluidized bed, *Chem. Eng. Res. Des.* 141 (2019) 220–228.
[16] D.H. Jiang, H.X. Zhang, X.F. Wang, Z.P. Zhu, X.Y. Cao, Influence of air staging on the operation characteristics of the CFB system, *J. Therm. Sci.* 32 (5) (2023) 1889–1898.
[17] J. Werther, E.U. Hartge, L. Ratschow, R. Wischnewski, Simulation-supported measurements in large circulating fluidized bed combustors, *Particuology* 7 (4) (2009) 324–331.
[18] C.H. Zheng, L.M. Cheng, X.L. Zhou, Q.S. Xu, Q.H. Wang, M.X. Fang, Z.Y. Luo, Numerical simulation of secondary air penetration depth in a 300 MW single-furnace circulating fluidized bed boiler, *J. Power Eng.* 29 (9) (2009) 801–805, 812.
[19] X. Zheng, J. Yan, J.P. Wang, X.F. Lu, Numerical study of the influence of secondary air uniformity on jet penetration and gas–solid diffusion characteristics in a large-scale CFB boiler, *Energies* 14 (18) (2021) 5679.
[20] C.K. Adams, Gas mixing in fast fluidised beds. Proceedings of the Second International Conference on Circulating Fluidized Beds, Compiégne, France, 1988, pp. 299–306.
[21] G. Amos, M.J. Rhodes, H. Mineo, Gas mixing in gas–solids risers, *Chem. Eng. Sci.* 48 (5) (1993) 943–949.
[22] R.J. Dry, C.C. White, Gas residence-time characteristics in a high-velocity circulating fluidised bed of FCC catalyst, *Powder Technol.* 58 (1) (1989) 17–23.
[23] A. Nautiyal, C.S. Chyang, P.W. Li, H.Y. Hou, Horizontal gas mixing in rectangular fluidized bed: a novel method for gas dispersion coefficients in various conditions and distributor designs, *Chin. J. Chem. Eng.* 25 (7) (2017) 848–861.
[24] J. Sternéus, F. Johnsson, B. Leckner, Characteristics of gas mixing in a circulating fluidised bed, *Powder Technol.* 126 (1) (2002) 28–41.
[25] J. Sternéus, F. Johnsson, B. Leckner, Gas mixing in circulating fluidised-bed risers, *Chem. Eng. Sci.* 55 (1) (2000) 129–148.
[26] F. Wei, Y. Jin, Z.Q. Yu, J.Z. Liu, Gas mixing in the cocurrent downflow circulating fluidised bed, *Chem. Eng. Technol.* 18 (1) (1995) 59–62.
[27] Y.H. Yang, X.L. Jia, F. Wei, Y. Jin, Hydrodynamics and lateral gas dispersion in a high-density circulating fluidized bed reactor with bluff internals, *Chin. J. Chem. Eng.* 9 (3) (2001) 291–296.
[28] B. Du, L.S. Fan, F. Wei, W. Warsito, Gas and solids mixing in a turbulent fluidized bed, *AIChE J.* 48 (9) (2002) 1896–1909.
[29] C.S. Chyang, Y.L. Han, C.H. Chien, Gas dispersion in a rectangular bubbling fluidized bed, *J. Taiwan Inst. Chem. Eng.* 41 (2) (2010) 195–202.
[30] J. Štefanica, J. Hrdlička, Experimental investigation of radial gas dispersion coefficients in a fluidized bed, *Acta Polytech* 52 (3) (2012) 97–100.
[31] Y.C. Lin, C.S. Chyang, Radial gas mixing in a fluidized bed using response surface methodology, *Powder Technol.* 131 (1) (2003) 48–55.
[32] M.L. Mastellone, U. Arena, The influence of particle size and density on the radial gas mixing in the dilute region of the circulating fluidized bed, *Can. J. Chem. Eng.* 77 (2) (1999) 231–237.
[33] Y.J. Cho, W. Namkung, S.D. Kim, S. Park, Effect of secondary air injection on axial solid holdup distribution in a circulating fluidized bed, *J. Chem. Eng. Jpn.* 27 (2) (1994) 158–164.
[34] M. Koksal, F. Hamdullahpur, Gas mixing in circulating fluidized beds with secondary air injection, *Chem. Eng. Res. Des.* 82 (8) (2004) 979–992.
[35] W. Namkung, S.D. Kim, Radial gas mixing in a circulating fluidized bed, *Powder Technol.* 113 (1–2) (2000) 23–29.
[36] W. Namkung, S.D. Kim, Gas backmixing in a circulating fluidized bed, *Powder Technol.* 99 (1) (1998) 70–78.
[37] C.Z. Yang, Y.F. Duan, H.T. Hu, Y.Q. Mao, P.P. Zhang, Characteristic of gas mixing in two-dimensional dual-leg fluidized bed, *CIESC J.* 63 (12) (2012) 3867–3874.
[38] H.R. Yang, J.F. Lu, G.X. Yue, Design theory of circulating fluidized bed boilers and determination of the design parameters, *J. Power Eng.* 26 (1) (2006) 42–48, 69.
[39] G.X. Yue, J.F. Lu, H. Zhang, H.R. Yang, J.S. Zhang, Q. Liu, Z. Li, E. Joos, P. Jaud, Design theory of circulating fluidized bed boilers, in: Proceedings of the 18th International Conference on Fluidized Bed Combustion, Toronto, Ontario, Canada, 2005, pp. 135–146.
[40] W.J. Massman, A review of the molecular diffusivities of H_2O, CO_2, CH_4, CO, O_3, SO_2, NH_3, N_2O, NO, and NO_2 in air, O_2 and N_2 near STP, *Atmos. Environ.* 32 (6) (1998) 1111–1127.